Properties of ^{187}Ta Revealed through Isomeric Decay

P. M. Walker,[1,*] Y. Hirayama,[2] G. J. Lane,[3] H. Watanabe,[4,5] G. D. Dracoulis,[3] M. Ahmed,[2,6] M. Brunet,[1] T. Hashimoto,[7] S. Ishizawa,[5,8,2] F. G. Kondev,[9] Yu. A. Litvinov,[10] H. Miyatake,[2] J. Y. Moon,[7] M. Mukai,[6,2,5] T. Niwase,[2,5,11] J. H. Park,[7] Zs. Podolyák,[1] M. Rosenbusch,[2] P. Schury,[2] M. Wada,[2,6] X. Y. Watanabe,[2] W. Y. Liang,[12] and F. R. Xu[12]

[1]*Department of Physics, University of Surrey, Guildford, GU2 7XH, United Kingdom*
[2]*Wako Nuclear Science Center (WNSC), Institute of Particle and Nuclear Studies (IPNS), High Energy Accelerator Research Organization (KEK), Wako, Saitama 351-0198, Japan*
[3]*Department of Nuclear Physics, RSPhys, Australian National University, Canberra, Australian Capital Territory 2601, Australia*
[4]*School of Physics, and International Research Center for Nuclei and Particles in Cosmos, Beihang University, Beijing 100191, China*
[5]*Nishina Center for Accelerator-Based Science, RIKEN, Wako, Saitama 351-0198, Japan*
[6]*University of Tsukuba, Tsukuba, Ibaraki 305-0006, Japan*
[7]*Rare Isotope Science Project, Institute for Basic Science (IBS), Daejeon 305-811, Republic of Korea*
[8]*Graduate School of Science and Engineering, Yamagata University, Yamagata 992-8510, Japan*
[9]*Physics Division, Argonne National Laboratory, Lemont, Illinois 60439, USA*
[10]*GSI Helmholtzzentrum für Schwerionenforschung, 64291 Darmstadt, Germany*
[11]*Department of Physics, Kyushu University, Nishi-ku, Fukuoka 819-0395, Japan*
[12]*School of Physics and State Key Laboratory of Nuclear Physics and Technology, Peking University, Beijing 100871, China*

(Received 24 July 2020; accepted 13 October 2020; published 6 November 2020)

Mass-separated $^{187}Ta_{114}$ in a high-spin isomeric state has been produced for the first time by multinucleon transfer reactions, employing an argon gas-stopping cell and laser ionization. Internal γ rays revealed a $T_{1/2} = 7.3 \pm 0.9$ s isomer at 1778 ± 1 keV, which decays through a rotational band with perturbations associated with the approach to a prolate-oblate shape transition. Model calculations show less influence from triaxiality compared to heavier elements in the same mass region. The isomer-decay reduced $E2$ hindrance factor $f_\nu = 27 \pm 1$ supports the interpretation that axial symmetry is approximately conserved.

DOI: 10.1103/PhysRevLett.125.192505

Progress in the study of heavy, neutron-rich nuclei is leading the way toward a deeper understanding of cosmic elemental abundances. For example, the $A \approx 195$ solar abundance peak is determined by the properties of unstable nuclei along the r-process (rapid neutron capture) path of stellar nucleosynthesis, which follows the $N = 126$ closed neutron shell up to $Z \approx 73$ [1]. Pinning down the structure of the $N \approx 126$ nuclei, and ultimately reaching the r-process path itself, are basic objectives of several new accelerator facilities, both planned and under construction [2–5]. Nevertheless, difficulties center on the low production rates and the lack of selective reaction mechanisms, so that additional experimental advances are needed [4,5]. A possibility for half-lives longer than about 100 ms is "isotope separation," where the nuclear reaction products are stopped, vaporized, ionized, mass separated, and transported to a low-background measurement station. However, the refractory chemistry of key elements, from hafnium ($Z = 72$) to iridium ($Z = 77$), makes them hard to vaporize [6]. An essential requirement is, therefore, to develop a suitable gas-stopping arrangement for the reaction products [7,8].

A promising additional feature of isotope separation is that it may be used with long-lived nuclear excited states (isomers) [9–11] whose γ-ray decay can enable the nuclear structure to be studied at high angular momentum, giving sensitivity to rotational and shape degrees of freedom. While the occurrence of sufficiently long-lived, high-spin isomers is rare [12], discoveries [13] in the Experimental Storage Ring (ESR) at GSI in Germany have opened a special opportunity in the neutron-rich hafnium and tantalum ($Z = 73$) isotopes.

We now report the first successful production and separation of low-energy beams of neutron-rich tantalum isotopes and isomers. The production process exploits multinucleon transfer (MNT) reactions which have been shown to be effective for making neutron-rich nuclei [14–16]. In the present work, the large angular momentum transfer in MNT reactions is a vital aspect for the formation of high-spin isomers. We focus on the internal decay of an isomer in ^{187}Ta, which reveals a perturbed rotational band and sheds light on the nuclear structure associated with a prolate-oblate shape transition.

The existence of ^{187}Ta was first established at GSI from high-energy projectile fragmentation of ^{197}Au [17].

Subsequently, it was observed with high mass resolution in the ESR using the same reaction. In the form of "bare" ions with all atomic electrons removed, the ^{187}Ta ground state (gs) and two isomeric states ($m1$ and $m2$) were identified and their masses and half-lives measured, yielding excitation energies of 1789 ± 13 and 2935 ± 14 keV, respectively [13]. The measured half-lives were 2.3 ± 0.6 min, 22 ± 9 s, and > 5 min for the gs, $m1$, and $m2$ states, respectively. Furthermore, without observing the decay radiations, it could be determined that there were both β and γ decays from the $m1$ isomer, but no other spectroscopic information was obtained. The key finding now reported is the detailed γ-ray decay pathway from the $m1$ isomer to the gs of ^{187}Ta. The first observation of γ rays following the β decay of the gs will be reported elsewhere, as will the tentative identification of decays associated with the $m2$ isomer.

The experiment was performed at the RIKEN Nishina Center in Saitama, Japan, with the recently commissioned KEK Isotope Separation System facility [18,19]. This is the first facility of its kind, capable of stopping heavy-ion reaction products in a high-pressure (80 kPa) argon gas cell, performing laser resonant ionization for element (Z) selectivity, and achieving mass (A) separation of the electrostatically extracted, singly charged, 20 keV ions in a dipole magnet with a resolving power $A/\Delta A = 900$. In the present work, the ^{187}Ta ions were produced by MNT reactions of a 50 particle-nA beam of ^{136}Xe at 7.2 MeV per nucleon, delivered by the RIKEN ring cyclotron. The beam was incident on a 5-μm-thick natural tungsten target (28% ^{186}W) at the entrance to the argon gas cell.

The 20 keV secondary beam of laser-ionized tantalum [20] was mass separated ($\approx$1.5 ions/s of ^{187}Ta) and transported to a moving-tape collection point, surrounded by a low-background, 32-element gas proportional counter with 80% of a 4π solid angle for β particles and conversion electrons [21], and four super Clover germanium γ-ray detectors with a total absolute full-energy-peak efficiency of 15% at 150 keV. In the analysis, $e-\gamma$ coincidences were always required, as they were very effective at removing background γ-ray events. Furthermore, the 32 elements of the gas counter were arranged in two concentric layers, and, by requiring events only in the first layer, isomeric cascades could be preferentially selected [19,21]. The tape transport was operated with equal beam-on and beam-off periods, with the radioactivity moved to a shielded location at the end of each cycle. The chosen beam-on periods were 30, 300, and 1800 s, with 5 days of data taking. During the beam-off periods at the $e-\gamma$ spectroscopy station, the beam was electrostatically deflected to a multireflection time-of-flight device for high-resolution mass analysis [22].

First, the $m1$ isomer half-life is discussed. The half-life derived from the ESR data for bare ions represents an upper half-life limit for neutral atoms, because conversion coefficients can be very large (greater than 100) for low-energy

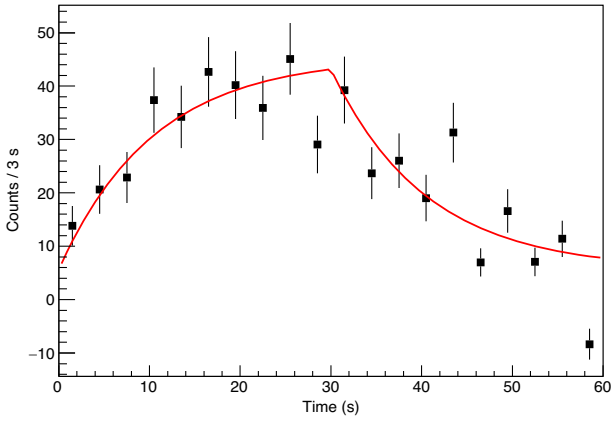

FIG. 1. Sum of γ-ray time spectra for transitions involved in the decay of ^{187}Ta^{m1}. The line through the data is a log-likelihood fit to the growth (beam on) and decay (beam off) periods, each of 30 s duration, yielding a half-life of 7.3 ± 0.9 s.

γ rays [23], yet electron conversion cannot take place in bare ions. Therefore, the present measurement searched for previously unassigned γ-ray transitions with $T_{1/2} \leq 22$ s. As illustrated in Fig. 1, transitions were identified that yielded a half-life of 7.3 ± 0.9 s. The time spectrum comes from the addition of the time evolution of ten different γ-ray transition intensities. For individual transitions, the half-life uncertainties are large, but by simple inspection of the time-gated γ-ray spectra it is clear that their half-lives are all less than 20 s, and no other ^{187}Ta half-lives of less than 1 min are known.

Having identified a number of γ-ray transitions associated with the relatively short half-life of 7.3 s, the γ-ray coincidence relationships ($\pm$300 ns) enabled them to be unambiguously ordered in a cascade, as shown in Fig. 2. The γ-ray sum-coincidence spectrum is illustrated in Fig. 3, where the tantalum x rays show that the isomer is undergoing internal decay. The level structure is independently confirmed by Gammasphere data from several years ago [24], also using MNT reactions, taken at the Argonne National Laboratory. Previously unplaced ^{187}Ta transitions and their coincidence relationships have now been

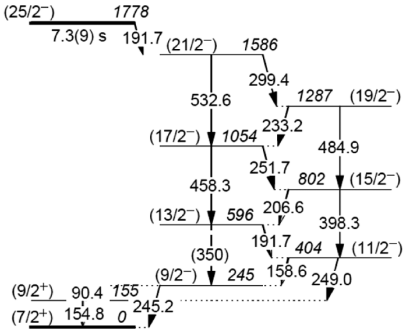

FIG. 2. Level scheme for ^{187}Ta obtained from the decay of its $T_{1/2} = 7.3 \pm 0.9$ s isomeric state at 1778 keV.

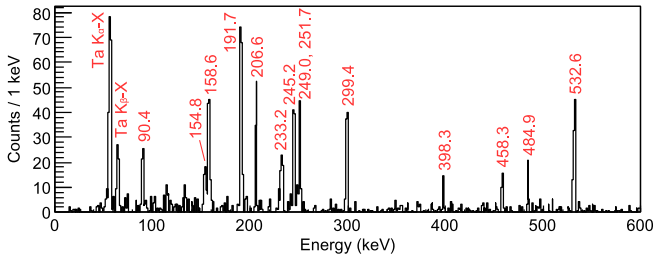

FIG. 3. Sum of γ-γ-coincidence energy spectra, illustrating transitions involved in the decay of $^{187}\mathrm{Ta}^{m1}$.

observed during the beam-off periods of the Gammasphere beam pulsing.

From the Gammasphere data, the γ-ray intensities, combined with theoretical conversion coefficients [23], enable the transition multipole characters to be deduced, assuming rotational properties for the band based on the 245 keV level. We discuss in more detail only the 191.7 keV doublet. It proved not to be possible to distinguish between the energies of these two transitions (with uncertainties of ± 0.5 keV), but their intensities can be separately determined. Thus, the conversion coefficient of the isomeric 191.7 keV transition is found to be $\alpha_T = 0.57 \pm 0.24$, which indicates $M1$ or $E2$ character. The theoretical conversion coefficients [23] are $\alpha_T = 0.07$, 0.69, 0.34, 3.72, and 2.69 for $E1$, $M1$, $E2$, $M2$, and $E3$, respectively. However, an $M1$ assignment would indicate the possibility of a competing $E2$ transition to the 1287 keV band member, which is unobserved. Therefore, a tentative $E2$ assignment is given for the isomeric 191.7 keV transition, and, hence, $I^\pi = (25/2^-)$ for the isomer itself.

Comparison with the ESR data [13] is instructive. Those data independently establish the energy difference between the isomer and the gs to be 1789 ± 13 keV, in good agreement with the present more-accurate value of 1778 ± 1 keV. The ESR measurements [13,25] also identified five β-decay events (as well as eight γ-decay events) from $^{187}\mathrm{Ta}^{m1}$, but, in the present work, no β-decay branch could be confirmed. Considering both datasets and that electron conversion is not possible for bare ions in the ESR, we estimate conservatively that the neutral atom has a β-decay branching ratio $< 40\%$.

The structure of the gs of ^{187}Ta is indicated by the systematic observation [26] that the gs of the lighter tantalum isotopes ($175 \leq A \leq 185$) is formed by the spin $I^\pi = \Omega^\pi = 7/2^+$, $7/2^+[404]$ Nilsson configuration, where Ω is the spin projection on the nuclear symmetry axis. The same configuration assignment for ^{187}Ta is supported in the present work by the observed β decay of the gs to states in ^{187}W. However, parentheses are used for all spin and parity assignments in Fig. 2 on account of the provisional gs assignment. The next-lowest intrinsic state is expected [26] to be the $9/2^-[514]$ configuration. This is entirely consistent with the observed structure, which is itself very similar to the corresponding structure in ^{185}Ta [24]. Once the gs spin and parity are taken to be $7/2^+$, as for the $7/2^+[404]$ configuration, all the other spins and parities in Fig. 2 are determined by the γ-ray intensities and implied conversion coefficients, as discussed above.

The isomer configuration comes from multiquasiparticle calculations. Reed *et al.* [13,25], assigned a $K^\pi = 27/2^+$ one-proton–two-neutron configuration $\{\pi 9/2^-[514] \otimes \nu 11/2^+[615] \otimes \nu 7/2^-[503]\}$, where K is the sum of the individual Ω values. This would be compatible with the deduced level scheme if the 191.7 keV transition from the isomer were of $E3$ character, but that is ruled out by the deduced conversion coefficient. We have performed two new sets of calculations with a Woods-Saxon potential and universal parameters [27], first multiconfiguration calculations [28–30] with fixed deformation [31], including residual interactions, and second configuration-constrained, potential-energy-surface (PES) calculations [32]. The calculations suggest two competing $K^\pi = 25/2^-$ configurations: $\{\pi 7/2^+[404] \otimes \nu 11/2^+[615] \otimes \nu 7/2^-[503]\}$ and $\{\pi 9/2^-[514] \otimes \nu 9/2^-[505] \otimes \nu 7/2^-[503]\}$, but we are unable to distinguish between them experimentally. The PES calculations give deformation parameters $(\beta_2, \gamma, \beta_4) = (0.208, 0°, -0.076)$ and $(0.189, 0°, -0.062)$, respectively. With regard to isomer decay rates (discussed later), the $\gamma = 0°$ axial symmetry is a significant feature.

Considering the rotational states populated by the isomer decay, it is instructive to analyze the $I \to I - 1$ transition energies. A rotational band with a constant moment of inertia, J, follows the well-known formula for the rotational energy $E_R = \hbar^2/2J[I(I+1) - K^2]$, so that the energy change $\Delta E(I \to I - 1)$ obeys the expression $\Delta E/2I = \hbar^2/2J$. In order to assess the regularity of a rotational band, it is common practice to plot this as a function of I, as shown in Fig. 4 for the $9/2^-[514]$ bands in ^{187}Ta, its isotope ^{185}Ta [24], and its isotone ^{189}Re [33]. For ^{185}Ta, the behavior is monotonic and slightly decreasing. This indicates a gently increasing moment of inertia, which is the normal behavior.

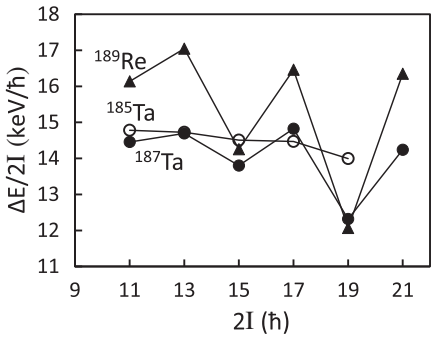

FIG. 4. Signature splitting as a function of angular momentum for $9/2^-[514]$ bands in ^{185}Ta [24], ^{187}Ta (this work), and ^{189}Re [33]. The energy ΔE is for $I \to I - 1$ transitions. Circles represent tantalum isotopes ($Z = 73$), and filled symbols represent $N = 114$ isotones.

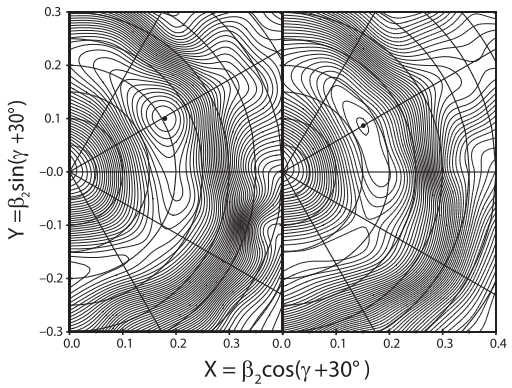

FIG. 5. TRS calculations for the $9/2^-[514]$ bands in ^{187}Ta (left) and ^{189}Re (right) at $\hbar\omega = 0.15$ MeV ($I \approx 5\hbar$). The energy minima (dots) are at $(\beta_2, \gamma, \beta_4) = (0.205, 0°, -0.079)$ for ^{187}Ta and $(0.174, 0°, -0.060)$ for ^{189}Re. Energy contours are at 200 keV intervals.

By contrast, there are significant oscillations, or "staggering," for ^{187}Ta, which become substantially larger in ^{189}Re. This staggering effect has recently been studied in the $9/2^-[514]$ bands of ^{187,189,191}Re, both experimentally and with triaxial particle-plus-rotor model calculations [33]. It was concluded that the triaxiality parameter (which ranges from $\gamma = 0°$ for prolate shape to 60° for oblate shape) takes values of 5°, 18°, and 25°, respectively, in the three rhenium isotopes. Since the staggering in the ^{187}Ta band is intermediate between that in ^{189}Re and ^{187}Re [33], it can be estimated that its triaxiality value is $\gamma \approx 10°$. It can also be observed in Fig. 4 that the $\Delta E/2I$ value is, on average, lower for ^{187}Ta than for ^{189}Re, indicating a higher moment of inertia for ^{187}Ta and, hence, a larger β_2 deformation.

In the present work, total Routhian surface (TRS) calculations [34–36] have been carried out for the $9/2^-[514]$ bands of ^{187}Ta and ^{189}Re. As illustrated in Fig. 5, these show axially symmetric, prolate minima. The minimum is shallower for ^{189}Re, and the contour lines extend in the axially asymmetric direction, particularly in the $\gamma < 0°$ direction. This is consistent with a greater role of axial asymmetry in ^{189}Re, relative to ^{187}Ta. Compared to the particle-plus-rotor calculations [33], the present work suggests the significant role of dynamic, rather than static, γ deformation at low spin. However, at high spin ($I \approx 18$), the TRS calculations show a dramatic change to oblate rotation, similar to that predicted in, for example, the hafnium isotopes [36].

An important aspect here is that $N \approx 116$ is the critical point for a *gs* prolate-oblate shape transition with an increasing neutron number. This has been well studied in the higher-Z elements, especially osmium ($Z = 76$) and platinum ($Z = 78$), where the prolate-oblate transition is achieved by passing through triaxial shapes [10,37–41]. However, calculations such as those of Robledo, Rodríguez-Guzmán, and Sarriguren [40] and the present work predict that, as Z decreases, the β_2 deformation increases and triaxiality plays a reduced role. We have here presented experimental evidence, through the reduced staggering behavior in the $9/2^-[514]$ band of ^{187}Ta, compared to that in its $N = 114$ isotone ^{189}Re, that this is indeed the case.

Further information about the triaxiality comes from the half-life of ^{187}Ta^{m1} ($T_{1/2} = 7.3 \pm 0.9$ s) which is long because the decay transition is "K forbidden," with $\Delta K > \lambda$, where ΔK is the change in K value and λ is the angular momentum carried by the transition. The degree of forbiddenness is defined as $\nu = \Delta K - \lambda$, and the reduced hindrance is $f_\nu = (T^\gamma_{1/2}/T^W_{1/2})^{1/\nu}$, where $T^\gamma_{1/2}$ is the partial γ-ray half-life and $T^W_{1/2}$ is the corresponding Weisskopf estimate [10]. In the present case of $E2$ decay from ^{187}Ta^{m1}, we find that $f_\nu = 27 \pm 1$, which is a substantial value [10,42]. However, compared to the $E2$ decay of ^{185}Ta^{m1}, with $f_\nu = 71$ [24], the $f_\nu = 27$ value indicates significant K mixing, qualitatively consistent with the greater staggering in the populated rotational band. Comparison with the equivalent $E2$ isomeric decay in ^{189}Re is not straightforward, because the branching intensities are not specified [33]. Nevertheless, a much smaller f_ν value is evident, indicating a substantial loss of axial symmetry. Therefore, this analysis supports the calculations ([40] and the present work) that show better axial symmetry for lower-Z elements in the $N \approx 116$ prolate-oblate shape transition region.

In summary, the excited-state structure of ^{187}Ta$_{114}$ has been revealed for the first time through its $m1$ isomer decay, with $T_{1/2} = 7.3 \pm 0.9$ s. Despite the close approach to $N \approx 116$, which is the critical point for the predicted *gs* prolate-oblate shape transition, the reduced hindrance for the $E2$ isomeric decay remains substantial, with $f_\nu = 27 \pm 1$, indicating that K is approximately conserved and, therefore, that axial symmetry is not strongly violated. Nevertheless, weak violation of axial symmetry is indicated by the observed staggering in the $9/2^-[514]$ rotational band that is populated through the isomer decay. Comparison with the rhenium isotone ^{189}Re supports calculations showing that axial symmetry is better conserved, through the $N \approx 116$ shape transition region, for the lower-Z nuclei. The new capability to produce low-energy beams of neutron-rich tantalum isotopes and isomers demonstrates the power of the gas-stopping technique for nuclear structure studies of exotic neutron-rich nuclei, even with refractory elements. This marks a milestone on the way to the exploration of nuclei predicted to have well-deformed oblate ground states and ultimately to $N \approx 126$ r-process nuclei.

This experiment was performed at the RI Beam Factory operated by RIKEN Nishina Center and CNS, University of Tokyo. The authors thank the RIKEN accelerator staff for their support. This work was funded in part by Grants

No. JP23244060, No. JP24740180, No. JP26247044, No. JP15H02096, No. JP17H01132, No. JP17H06090, and No. JP18H03711 from JSPS KAKENHI; No. ST/L005743/1 from United Kingdom STFC; No. 11921006 and No. 11835001 from NSFC; No. 682841 "ASTRUm" from ERC (Horizon 2020); and No. DE-AC02-06CH11357 from U.S. Department of Energy (Office of Nuclear Physics).

*p.walker@surrey.ac.uk

[1] T. Kajino and G. Mathews, Rep. Prog. Phys. **80**, 084901 (2017).
[2] D. Geesaman *et al.*, The 2015 long range plan for nuclear science, U.S. Department of Energy, Office of Science report, 2015.
[3] A. Bracco *et al.*, NuPECC long range plan 2017 perspectives in nuclear physics, European Science Foundation report, 2017.
[4] T. Kajino, W. Aoki, A. B. Balantekin, R. Diehl, M. A. Famiano, and G. J. Mathews, Prog. Part. Nucl. Phys. **107**, 109 (2019).
[5] C. J. Horowitz *et al.*, J. Phys. G **46**, 083001 (2019).
[6] U. Köster *et al.*, Eur. Phys. J. Spec. Top. **150**, 285 (2007).
[7] Y. Hirayama *et al.*, Nucl. Instrum. Methods Phys. Res., Sect. B **353**, 4 (2015).
[8] G. Savard, M. Brodeur, J. A. Clark, R. A. Knaack, and A. A. Valverde, Nucl. Instrum. Methods Phys. Res., Sect. B **463**, 258 (2020).
[9] P. M. Walker and G. D. Dracoulis, Nature (London) **399**, 35 (1999).
[10] G. D. Dracoulis, P. M. Walker, and F. G. Kondev, Rep. Prog. Phys. **79**, 076301 (2016).
[11] P. M. Walker and Zs. Podolyák, Phys. Scr. **95**, 044004 (2020).
[12] A. K. Jain, B. Maheshwari, S. Garg, M. Patial, and B. Singh, Nucl. Data Sheets **128**, 1 (2015).
[13] M. W. Reed, I. J. Cullen, P. M. Walker, Yu. A. Litvinov, K. Blaum *et al.*, Phys. Rev. Lett. **105**, 172501 (2010).
[14] Y. X. Watanabe, Y. H. Kim, S. C. Jeong, Y. Hirayama, N. Imai *et al.*, Phys. Rev. Lett. **115**, 172503 (2015).
[15] C. Li, X. Xu, J. Li, G. Zhang, B. Li, C. A. T. Sokhna, Z. Ge, F. Zhang, P. Wen, and F.-S. Zhang, Phys. Rev. C **99**, 024602 (2019).
[16] V. V. Desai, W. Loveland, R. Yanez, G. Lane, S. Zhu, A. D. Ayangekaa, J. P. Greene, F. G. Kondev, R. V. F. Janssens, and P. A. Copp, Eur. Phys. J. A **56**, 150 (2020).
[17] J. Benlliure, K.-H. Schmidt, D. Cortina-Gil, T. Enqvist, F. Farget, A. Heinz, A. R. Junghans, J. Pereira, and J. Taieb, Nucl. Phys. **A660**, 87 (1999).
[18] Y. Hirayama *et al.*, Nucl. Instrum. Methods Phys. Res., Sect. B **463**, 425 (2020).
[19] Y. X. Watanabe *et al.*, Phys. Rev. C **101**, 041305(R) (2020).
[20] Y. Hirayama, M. Mukai, Y. X. Watanabe, M. Oyaizu, S. C. Jeong, Y. Kakiguchi, P. Schury, M. Wada, and H. Miyatake, Rev. Sci. Instrum. **90**, 115104 (2019).
[21] M. Mukai *et al.*, Nucl. Instrum. Methods Phys. Res., Sect. B **463**, 421 (2020).
[22] P. Schury *et al.* (to be published).
[23] T. Kibédi, T. W. Burrows, M. B. Trzhaskovskaya, P. M. Davidson, and C. W. Nestor, Nucl. Instrum. Methods Phys. Res., Sect. A **589**, 202 (2008).
[24] G. J. Lane, G. D. Dracoulis, A. P. Byrne, R. O. Hughes, H. Watanabe *et al.*, Phys. Rev. C **80**, 024321 (2009).
[25] M. W. Reed, P. M. Walker, I. J. Cullen, Yu. A. Litvinov, D. Shubina *et al.*, Phys. Rev. C **86**, 054321 (2012).
[26] A. K. Jain, R. K. Sheline, P. C. Sood, and K. Jain, Rev. Mod. Phys. **62**, 393 (1990).
[27] S. Cwiok, J. Dudek, W. Nazarewicz, J. Skalski, and T. Werner, Comput. Phys. Commun. **46**, 379 (1987).
[28] K. Jain, O. Berglin, G. D. Dracoulis, B. Fabricius, N. Rowley, and P. M. Walker, Nucl. Phys. **A591**, 61 (1995).
[29] F. G. Kondev, G. D. Dracoulis, A. P. Byrne, T. Kibédi, and S. Bayer, Nucl. Phys. **A617**, 91 (1997).
[30] D. J. Hartley *et al.*, Phys. Rev. C **101**, 044301 (2020).
[31] P. Möller, A. J. Sierk, T. Ichikawa, and H. Sagawa, At. Data Nucl. Data Tables **109–110**, 1 (2016).
[32] F. R. Xu, P. M. Walker, J. A. Sheikh, and R. Wyss, Phys. Lett. B **435**, 257 (1998).
[33] M. W. Reed *et al.*, Phys. Lett. B **752**, 311 (2016).
[34] W. Satula, R. Wyss, and P. Magierski, Nucl. Phys. **A578**, 45 (1994).
[35] W. Satula and R. Wyss, Phys. Scr. **T56**, 159 (1995).
[36] F. R. Xu, P. M. Walker, and R. Wyss, Phys. Rev. C **62**, 014301 (2000).
[37] D. Cline, Annu. Rev. Nucl. Part. Sci. **36**, 683 (1986).
[38] C. Y. Wu *et al.*, Nucl. Phys. **A607**, 178 (1996).
[39] J. Jolie and A. Linnemann, Phys. Rev. C **68**, 031301(R) (2003).
[40] L. M. Robledo, R. Rodríguez-Guzmán, and P. Sarriguren, J. Phys. G **36**, 115104 (2009).
[41] K. Nomura, T. Otsuka, R. Rodríguez-Guzmán, L. M. Robledo, and P. Sarriguren, Phys. Rev. C **84**, 054316 (2011).
[42] F. G. Kondev, G. D. Dracoulis, and T. Kibédi, At. Data Nucl. Data Tables **103–104**, 50 (2015).